Physica Scripta. T92, 467–470, 2001

Slow Highly Charged Ion Facility at RIKEN

Y. Kanai[1]*, D. Dumitriu[1], Y. Iwai[1,2], T. Kambara[1], T. M. Kojima[1], A. Mohri[1], Y. Morishita[1], Y. Nakai[1], H. Oyama[1], N. Oshima[1] and Y. Yamazaki[1,2]

[1] Atomic Physics Lab., RIKEN, Wako, Saitama 351-0198, Japan
[2] Institute of Physics, Graduate School of Arts and Sciences, University of Tokyo, Meguro, Tokyo 153-8902, Japan

Received August 20, 2000; accepted December 19, 2000

PACS Ref: 39.90.+d, 07.77.Ka

Abstract

To study collision processes of slow and ultra-slow highly charged ions (HCI) with atoms, molecules, and surfaces, we have been constructing a slow highly charged ion facility at RIKEN. A 14.5 GHz Caprice type ECR ion source (ECRIS) is used as the primary ion source of the facility. At present, the energy of the ion beam from the ECRIS ranges from 10 eV/q to 20 keV/q, where q is the charge state of the ions. In order to further reduce the energy (< 1 eV/q), we are developing two different schemes, which is one of the most important feature of the facility. The two schemes are (1) a positron cooling of HCIs and (2) a multiple ionization of neutral atoms or singly-charged ions with a femtosecond (fs) Tera-Watt (TW) laser. This paper presents an overview of the present facility and the schemes to produce ultra-slow HCI beams, which are expected to open new research fields.

1. Introduction

Collision processes of slow highly charged ions (HCI) with atoms, molecules, and surfaces have been intensively studied in the last decade [1,2]. "Slow" referred above means that the collision velocity is smaller than that of active electrons participating in the collision. In this energy region, precise measurements have been done with various experimental techniques [2–7]. When the collision energy becomes even lower, the collision processes of HCI with atoms, molecules, and surfaces show qualitatively different features as follows:

(1) The Langevin orbiting processes due to the attractive induced dipole polarization become predominant in the charge transfer processes. The Langevin cross section is given by $\sigma_L = \pi[4\alpha q^2/\mu v^2]^{1/2}$, where α is the dipole polarizability of the target, q the charge state of the projectile ion and v the collision velocity, μ the reduced mass of the collision system. Since the Langevin cross section is proportional to q/v, this effect enhances the charge transfer cross section at low energies (< 1 eV/q) in the HCI collisions [7].
(2) In ion-solid interaction, one of the most important parameters is energy deposition, which is normally governed by the kinetic energy (K) of the projectile. In the case of slow HCIs, their potential energy (U) is expected to play an important role. A zeroth order criterion of the potential energy dominant region may naturally be given by $U > K$, where the effect of the potential energy can be clearly seen [8–10].

In order to study this new frontier of HCI collisions with mono-energetic very low and ultra low energy HCI beams, we have been constructing the slow highly charged ion facility at RIKEN. In the next section, we will overview the facility, and then explain the plan to produce ultra slow/cold HCIs.

2. Overview of the facility

A layout of the facility is shown in Fig. 1. The facility consists of three parts:

(1) A 14.5 GHz Electron Cyclotron Resonance Ion Source (ECRIS) and four slow HCI beam lines.
(2) An electro-magnetic trap for the production of ultra slow HCIs.
(3) A fs TW laser to produce HCIs.

The HCI beam is extracted from the ECRIS and momentum analyzed by an analyzing magnet (AM). The HCI beam is then focused by a magnetic quadrupole triplet lens and delivered to one of the four beam lines by a switching magnet (SW). Typical ion currents from the ECRIS, which are measured after the analyzing magnet, are listed in Table I.

BL 1 is for soft X-ray beam-capillary spectroscopy (BCS) [11–13] of meta-stable states. To transfer slow HCI (> 10 eV/q) with high efficiency, the HCI are transported through a floated beam line at 5 keV/q, and then decelerated and focused by a lens system just in front of the capillary. In this case, the energy spread of the beam is primarily determined by the intrinsic energy width of the ions from the ECRIS, which is typically a few eV/q. Figure 2 shows

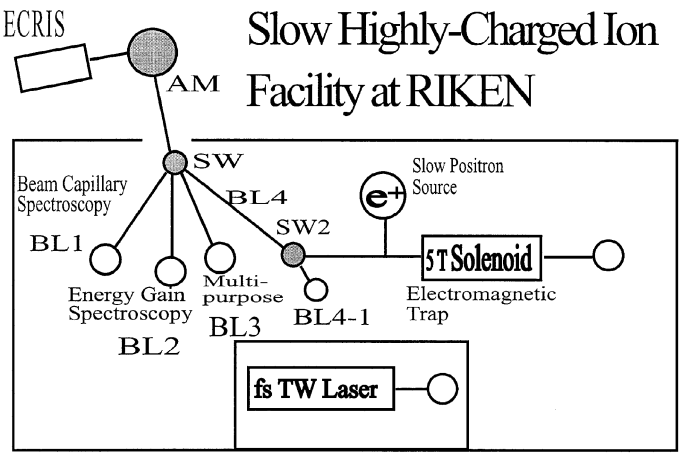

Fig. 1. Layout of the Slow Highly Charged Ion Facility.
HCI beams from the ECRIS are delivered to three experimental setups (BL1 to 3) and to the HCI trap (BL4). AM: analyzing magnet, SW, SW2: switching magnet. The BL4-1 is now under preparation for the BCS experiment.

*e-mail: kanai@rarfaxp.riken.go.jp

Table I. *Typical Ion Currents from ECRIS measured after AM. Extraction voltage 15 kV. Aluminum plasma chamber is used. Beam size at Faraday cup is 15 mm × 15 mm.*

Ions	O^{3+}	O^{5+}	O^{6+}	O^{7+}	Ar^{8+}	Ar^{11+}	Ar^{14+}	Ar^{16+}
Currents (μA)	740	232	330	60	291	68	3.5	0.12

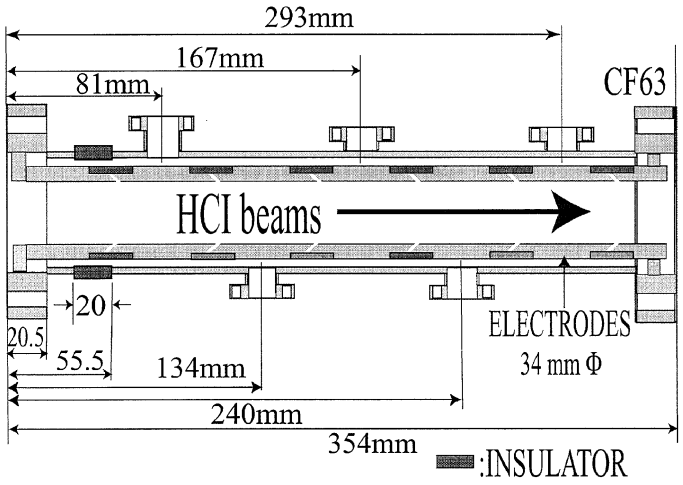

Fig 2. A schematic drawing of Deceleration Lens at BL1.

the deceleration lens of BL1, which consists of 7 cylindrical electrodes of 34 mm inner diameter. The available energy range at BL1 is from 10 eV/q to 20 keV/q.

BL2 is for experiments with mono-energetic slow HCIs. It consists of a deceleration lens followed by a double path hemispherical analyzer of 40 mm radius. The deceleration lens consists of 6 disk electrodes with 40 mm inner diameter, which works as a highly-efficient first deceleration stage of HCIs from 2–5 keV/q down to 300 eV/q. The 300 eV/q HCIs are further decelerated by a second deceleration lens down to the final energy, and then monochromatized with the double path hemispherical analyzer having an energy resolution of $\Delta E/E = 1/150$ [14,15]. Four jaw slits between the two deceleration stages, and two apertures of 1 mm diameters at the entrance lens of the hemispherical analyzer are used to limit the angular divergence to $\sim 1^\circ$. Typical currents after the analyzer are listed in Table II. A single-path 50 mm radius hemispherical electrostatic energy analyzer with $\Delta E/E = 1/100$ is installed on a turntable in the chamber, which allows double differential energy gain spectroscopy.

Table II. *Typical Ion Currents below 100 eV/q. High voltage of –2 kV is applied to the beam line. The ion intensities are measured after the deceleration and energy analysis. Typical beam size is a few mm at Faraday cup in the chamber of BL2.*

Ions	Ar^{4+}	Ar^{6+}	Ar^{8+}	He^{+}	He^{2+}
Energy (eV)	240	270	280	20	140
Energy Width (eV)	2.7	1.5	1.6	0.18	1.16
Intensity (10^8 s^{-1})	8.4	7.5	1.4	0.4	15.6

BL3 is a plain (i.e. no deceleration mechanism) beam line for various *ad hoc* experiments [16]. The available energy of HCIs is from 1 keV/q to 20 keV/q.

BL4 is newly prepared particularly for preparation of ultra slow HCIs. The HCIs from the ECRIS are transported to the electro-magnetic trap through BL4 and a second switching magnet (SW2). The available energy at BL4 is from 1 keV/q to 20 keV/q. The HCIs injected into the trap are sympathetically cooled with cold positron plasmas pre-injected in the trap. Details of the cooling scheme in the trap will be discussed in the next section [17]. At BL4-1 which is another beam line after SW2, a visible light BCS experiment is under preparation which will provide information on the very beginning of the charge transfer in HCI-surface collisions [13,18]

In parallel to the production of positron-cooled ultra slow HCIs, a fs TW laser is prepared (see Fig. 1) to study the production mechanisms of HCIs under strong electric fields, which is known to produce multiple ionization of atoms, molecules, and clusters [19–21]. The production mechanisms are not well-understood [22].

3. Cold HCI production

3.1. *Positron cooled HCI*

HCIs from the ECRIS are injected through the beam line (BL4) into a strong magnetic field where an electromagnetic trap is installed. The HCIs are cooled with a cold positron plasma in the trap [17]. The procedure is an inverted version of antiproton cooling with electrons [23], which is going on at CERN to produce strong ultra slow antiproton beams [24–26]. The HCIs will be cooled down to the environmental temperature (several Kelvin), which are then extracted from the trap to study, e.g., HCI-surface interaction.

Figure 3 shows the cooling procedure of HCIs, which is divided into several stages as described below.

Step 1: Electron accumulation and cooling.
Electrons are injected and accumulated in the trap with electric potential gates on both ends of the trap, which confines the axial motion of the electrons. On the other hand, the magnetic field of the solenoid confines the electrons radially. Electrons are cooled down by synchrotron radiation due to a strong magnetic field (5T) within a fraction of a second.

Step 2: Positron accumulation and cooling.
Positrons of keV energies are injected into the trap area and converted into a few eV positrons with a tungsten (W) re-moderator, sympathetically cooled with the cold electron plasmas and then trapped, and then further cooled via synchrotron radiation. Assuming a re-moderator efficiency of 25% [27] and a slow positron intensity of 10^7 positrons/second, about 10^8 positrons are to be accumulated in the trap within 100 seconds.

Step 3: HCI injection and cooling by collisions with cold positrons.
A simulation tells us that 10^6 of 2 keV/q Ar^{8+} are cooled down to 100 K by collisions with the 10^8 cold positrons within 10 seconds as shown in Fig. 4 [17]. In this simulation, the time dependences of temperatures for positrons and HCIs are calculated by the

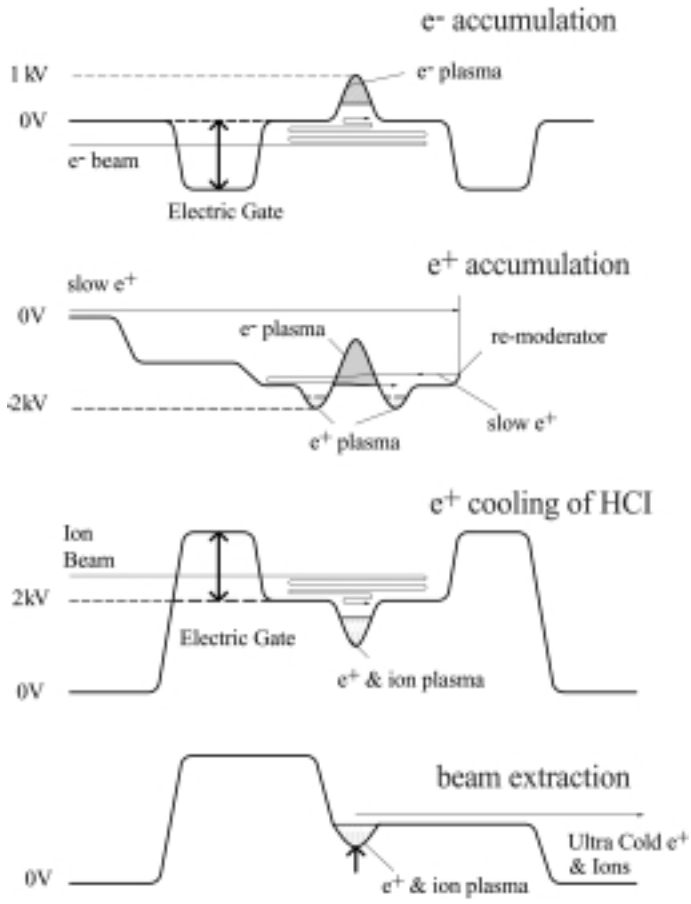

Fig. 3. Electric potential configuration in the electromagnetic trap.

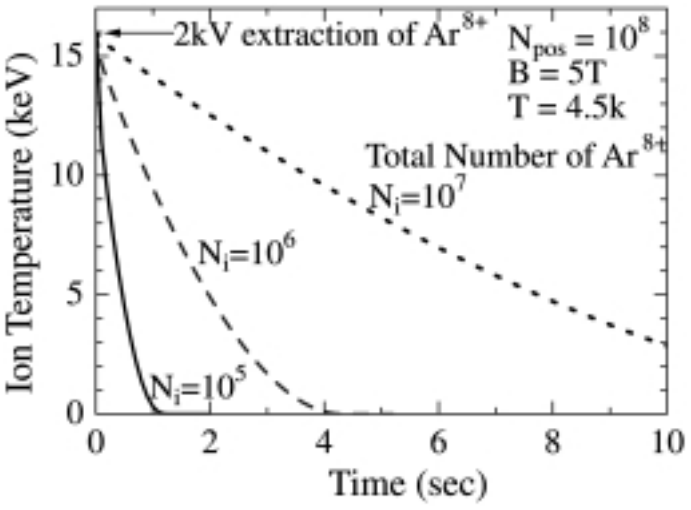

Fig. 4. Simulation of positron cooling.
The number of positrons in the trap is assumed to be 10^8 with their temperature of 4.5 K. The solid, broken, and dotted lines show the time dependences of the ion temperature for 10^5, 10^6, and 10^7 Ar^{8+} ions of 16 keV, respectively.

following rate equations,

$$\frac{\mathrm{d}}{\mathrm{d}t}T_\mathrm{i} = -\frac{1}{\tau_\mathrm{eq}}(T_\mathrm{i} - T_{\mathrm{e}+}), \tag{1}$$

$$\frac{\mathrm{d}}{\mathrm{d}t}T_{\mathrm{e}+} = \frac{N_\mathrm{i}}{N_{\mathrm{e}+}}\frac{1}{\tau_\mathrm{eq}}(T_\mathrm{i} - T_{\mathrm{e}+}) - \frac{2}{3\cdot\tau_\mathrm{c}}(T_{\mathrm{e}+} - T_0), \tag{2}$$

where, N_i and $N_{\mathrm{e}+}$ are the total number of HCIs and positrons sharing the same volume, and T_i, $T_{\mathrm{e}+}$, and T_o the temperatures of HCIs, positrons, and the environment, respectively, τ_c a cooling time constant of the synchrotron radiation, e.g., 0.1 s in a magnetic field of 5 T. τ_eq is a time constant for thermal equilibration of both positrons ($T_{\mathrm{e}+}$) and HCIs (T_i) and is given by

$$\tau_\mathrm{eq} = \frac{3\cdot 2^{1/2}\pi^{3/2}\varepsilon_0^2 m_\mathrm{i} m_{\mathrm{e}+} k^{3/2}}{n_{\mathrm{e}+} z^2 e^4 \ln\Lambda}\left(\frac{T_{\mathrm{e}+}}{m_{\mathrm{e}+}} + \frac{T_\mathrm{i}}{m_\mathrm{i}}\right)^{3/2} \tag{3}$$

where ε_o is the permittivity of vacuum, k the Boltzmann constant, m_i the mass of HCI, $m_{\mathrm{e}+}$ the mass of the positron, $n_{\mathrm{e}+}$ the positron density, z the charge states of HCI, e the electron charge, ln Λ the Coulomb logarithm [28]. Λ is defined as the ratio of the Debye length to the closest approach between positrons and HCIs.

Step 4: Extraction of ultra slow HCI from the trap.
The expectation values of intensity of the cold HCI are 10^6 particles/one cooling-cycle, i.e. 2 min, under the conditions listed in Tables III and IV.

The positrons are generated by a ^{22}Na radioactive source. Energetic positrons from the ^{22}Na are efficiently degraded in a Ne gas solid moderator prepared just in front of the ^{22}Na source [29] with an efficiency of $\sim 0.5\%$, are then accelerated to ~ 100 eV and guided by a 10 mT magnetic field to the trap area. The specifications of the positron source are summarized in Table III.

A superconducting solenoid of 5 T is prepared to cool electrons and positrons, and also to stably trap slow HCIs, the system parameters of which are given in Table IV.

3.2. *TW-Laser*

Multiple ionization processes induced by the fs TW laser will be used to produce slow HCIs as another method. Table V gives a specification of the laser. To obtain enough power density to produce HCIs, the laser beam with 40 mm diameter is introduced into a vacuum chamber via a fused-silica glass window, and then focused by an off-axis parabolic

Table III. *Specification of the slow positron source.*

Positron Source:	^{22}Na (40 mCi)
Moderator:	Rare Gas Solid (Ne)
Moderation Efficiency:	0.5%
Beam Intensity:	5×10^6 slow e^+/s
Energy Spread:	3 eV
Beam Diameter:	5 mm (at moderator)
Beam Transport:	Magnetic Transport (10 mT)

Table IV. *Specification of the superconducting solenoid for the electromagnetic trap.*

Magnetic Field (B):	< 5 Tesla
$\Delta B/B$ in trap region:	$< 10^{-3}$
Expected Trap Region:	4 mm in diameter $\times$500 mm in length
Vacuum Vessel Inner Diameter:	96 mm
Inner Wall Temperature:	6 K

Table V. *Specifications of the fs TW laser.*

Wave Length:	780 nm
Energy:	250 mJ
Beam Diameter:	40 mm
Repetition Rate:	10 Hz

mirror down to about 40 microns in diameter. The power density at the target position is about $10^{17}\,W/cm^2$. A Coulomb-barrier suppression model [30] predicts that this power density is strong enough to produce, e.g., Ne^{6+} and Ar^{8+} ions. In the first stage of the experiment, the production mechanism of HCI with a fs TW laser will be studied with so-called COLTRIMS (Cold Target Recoil Ion Momentum Spectroscopy) technique [3].

One of the peculiar aspects of the TW laser induced multiple ionization is literally its short production time (100 fs). This has the distinguished advantage to produce highly charged ions of short lifetime radio isotopes. Actually a Radio Isotope Beam Factory (RIBF) is under construction at RIKEN, which will start its operation from year 2003, where various RI beams of several 100 MeV/u are available with projectile fragmentation technique. We are currently developing a high efficient RI ion guide system to decelerate the above RI beam down to a few eV [31]. The singly-charged slow RI ions thus produced will be introduced into an ion trap for high precision laser spectroscopy, or into a Penning trap after multiple ionization with a TW laser for high precision q/m measurements.

References

1. For example, see "Proc. IX International Conference on the Physics of Highly Charged Ions, Bensheim, Sept. 9–14, 1998", in Physica Scripta **T80** (1999).
2. Morgenstern, R., Schlathoelter, T. and Hoekstra, R., "The Physics of Electronic and Atomic Collisions", (Eds Y. Itikawa, K. Okuno, H. Tanaka, A. Yagishita and M. Matsuzawa), (AIP Conference Proceedings 500, 1999) p. 65, and references therein.
3. Cassimi, A., Physica Scripta **T80**, 98 (1999), and references therein.
4. Shiromaru, H. *et al.*, Physica Scripta **T80**, 110 (1999).
5. Briand, J.-P. *et al.*, Phys. Rev. Lett. **65**, 159 (1990).
6. Stolterfort, N. *et al.*, Phys. Rev. Lett. **57**, 74 (1986).
7. Okuno, K., Saitoh, H., Soejima, K., Kravis, S. and Kobayashi, N., "The Physics of Electronic and Atomic Collisions", (Eds. L. J. Dube, J. B. Mitchell, J. W. McConkey and C. E. Brion), (AIP Conference Proceedings 360, 1995), p. 867.
8. Kakutani, K., Azuma, T., Yamazaki, Y., Komaki, K. and Kuroki, K., Jpn. J. Appl. Phys. **34**, L580 (1995).
9. Okabayashi, N. *et al.*, Physica Scripta **T80**, 555 (1999).
10. Neidhart, T. *et al.*, Phys. Rev. Lett. **74**, 5280 (1995).
11. Hutton, R. *et al.*, in "Abstracts of 21st ICPEAC, Sendai, July 22–27, 1999", p. 705.
12. Thuriez, S. *et al.*, in "Abstracts of 21st ICPEAC, Sendai, July 22–27, 1999", p. 706.
13. Yamazaki, Y., Int. J. Mass Spectrom. **192**, 437 (1999), and references therein.
14. Kitajima, M., Nakai, Y., Kanai, Y., Yamazaki, Y. and Itoh, Y., Physica Scripta **T80**, 377 (1999).
15. Hoshino, M. *et al.*, Physica Scripta, this issue.
16. Ogura, K. *et al.*, in "Abstracts of 21st ICPEAC, Sendai, July 22–27, 1999", p. 747.
17. Oshima, N. *et al.*, in "Proc. Int. Workshop on Advanced Technique of Positron Beam Generation and Control, Wako, December 16–18, 1998", p. 64.
18. Morishita, Y. *et al.*, Physica Scripta **T80**, 212 (1999).
19. Fittinghoff, D. N., Bolton, P. R., Chang, B. and Kulander, K. C., Phys. Rev. Lett. **69**, 2642 (1992).
20. McPherson, A. *et al.*, Phys. Rev. Lett. **72**, 1810 (1994).
21. Ditmire, T., Donnelly, T., Rubenchik, A. M., Falcone, R. W. and Perry, M. D., Phys. Rev. A **53**, 3379 (1996).
22. Moshammer, R. *et al.*, Phys. Rev. Lett. **84**, 447 (2000).
23. Gabrielse, G. *et al.*, Phys. Rev. Lett. **63**, 1360 (1989).
24. Yamazaki, Y., Nucl. Instrum. Meth. B **154**, 174 (1999).
25. Yamazaki, Y., "Non-Neutral Plasma Physics III", (Eds J. Bollinger *et al.*, AIP Press, 1999) p. 48.
26. Ichioka, T. *et al.*, "Non-Neutral Plasma Physics III", (Ed J. Bollinger *et al.*, AIP Press, 1999) p. 59.
27. Schultz, P. and Lynn, K. G., Rev. Mod. Phys. **60**, 701 (1988).
28. Spitzer, L., "Physics of Fully Ionized Gases", (Interscience Publishers Inc. New York, 1962).
29. Murphy, T. J. and Surko, C. M., Phys. Rev. A **46**, 5696 (1992).
30. Augst, A., Meyerhofer, D. D., Strickland, D. and Chin, S. L., J. Opt. Soc. Am. B **8**, 858 (1991).
31. Wada, M. *et al.*, Hyperfine Interactions **103**, 59 (1996).